Mansoura Engineering Journal

Volume 32 | Issue 2 Article 17

12-8-2020

Nonlinear Panel Flutter Analysis at High Supersonic Speed.

S. Abou-Amer
Vice Dean of AHI for management & Informatics

A. Dahshan
Hairman of AHI for management & Informatics

M. El Nomrossy
Chairman of Aerospace Research Center, AO1. Senior Member of AIAA

Mansoura Engineering Journal, (MEJ), Vol. 32, No. 2, June 2007. M. 21

Nonlinear Panel Flutter Analysis at High Supersonic Speed

التحليل اللاخطى لرفرفة الألواح عند السرعات أعلى من سرعة الصوت

ABOU-AMER S. A. *, DAHSHAN A. M. **, & EL NOMROSSY M. ***

* Vice Dean of AHI for management & Informatics
** Chairman of AHI for management & Informatics
*** Chairman of Aerospace Research Center, AOI. Senior Member of AIAA

الخلاصة

تتعرض الألواح الخارجية المكونة للكساء الخارجى للمركبات التى تطير بسرعات أعلى من سرعة الصوت فى الغلاف الخارجى لما يسمى بالإهتزازات المثارة ذاتيا من النوع ذو الترددات المحدودة. إن الرفرفة التى تحدث لهذه الألواح تنتج من عدم الإتزان الينامكى للقوى الإيروديناميكية وقوى القصور الذاتى وكذا قوى المرونة للألواح.

تم سياق معدلات الحركة للألواح فى حالة الرفرفة مستخدمين نظرية فان كارمن الخاصة للألواح فى حالة الإنحناءات الكبيرة بالإضافة إلى النظرية الإيروديناميكية الخطية لسيال الهواء المنتظم على سطح الكساء. إن هذه المعادلات تم سياقها كدالة فى الإزاحة العمودية فى شكل لا بعدى. وبإستخدام طريقة جالركن تم تحويل هذه المعادلات جزئية التفاضل اللاخطية إلى معادلات عادية التفاضل اللاخطية فى متغير واحد هو الزمن. وتم حل هذه المعادلات بطريقة الإتزان الهارمونى ونيوتن رافسون. تم مقارنة النتائج الحل النظرى مع النتائج المعملية فى بعض المراجع المنشورة ووجدت متطابقة.

بعد الإطمئنان على النموذج الرياضى المستخدم تم عمل دراسة بارامترية للعوامل المؤثرة على ظاهرة الرفرفة للألواح مثل الخمد الإيروديناميكى والخمد الهيكلى والأحمال فى الإتجاه الطولى والعرضى للألواح والأحمال الحرارية وأخيرا تأثير الضغط الموجود فى الفراغ الموجود تحت الألواح.

Abstract

Exterior panels forming the exterior skin of flight vehicles traveling through the atmosphere at high supersonic speeds are often susceptible to the occurrence of limit-cycle type self- excited vibrations called flutter. Panel flutter is resulting from the dynamic instability of the aerodynamic, inertia, and elastic forces of the system.

The equation of motion for panel flutter are derived using Von Karman's large deflection plate theory and quasi-steady aerodynamic theory. The equations are given in terms of the displacement and are presented in non-dimensional form. Galerkins method is used to transform the system of nonlinear partial differential equations into a system of nonlinear ordinary differential equations in time variable. The obtained equations are then solved by the method of harmonic balance and Newton-Raphson algorithm. The results are compared with both theoretical and experimental results given in publications.

Then, a parametric study is performed to study the effects of aerodynamic loading, aerodynamic damping, structural damping, in-plane applied loads, thermal stresses and cavity pressure.

Keywords

Panel Flutter; Aerodynamic Loading; Aerodynamic Damping; Structural Damping; Cavity Effect; Thermal Effect; Von Karman's Large Deflection Plate Theory; Quasi-Steady Aerodynamic Theory; Galerkins Method; Newton-Raphson Algorithm; Harmonic Balance Method.

Accepted May 27, 2007

I. Introduction:

Panel flutter results from the interaction between the panel and the flow pressure forces brought about by the panel motion. This causes a loss of the stability of the panel in its un-deformed shape, so that any disturbance applied to it leads to oscillations of growing amplitude. Thus, it is a self excited oscillation resulting from the dynamic instability of the aerodynamic, inertia, and elastic forces of the system. This growth is limited, however, by the membrane tension stresses induced in the panel by the flutter motion itself. The result of this self-limiting action is a sustained oscillation of constant amplitude, called limit-cycle motion. There are many variables that affect panel flutter and a major problem involved in the study of panel flutter is the isolation and determination of the significance of these variables. The flutter boundary for a particular panel is a complex function of such variables as panel configuration, mid-plane stress, edge restraint, flow angularity, dynamic pressure, Mach number, pressure differential, structural damping, aerodynamic damping, and finally the boundary layer thickness. Due to the complexity of panel flutter, most theoretical studies make use of simplified assumptions, see Ref [20]. However these assumptions are usually so restrictive that the theoretical model does not accurately represent realistic conditions. In fact it is found that the application of the exact aerodynamic theory does not remove the discrepancies that presently exist between theory and experiment for flutter of stressed panels. The inclusion of structural damping is found to have a large effect in some instances and can tend to eliminate some of the differences.

There are certain unifying features common to all aeroelastic problems which provide a convenient framework for introducing and classifying the entire subject. These features include the casting of the aeroelastic equations in an operator form and the generalized solution of such operator equations, see Ref. [1]. Investigation of the theoretical foundations, methods of analysis for treating linear aeroelastic models, their nonlinear counterparts, and the requisite aerodynamic theory were discussed, with the three levels of approximation to the motion dependent aerodynamic pressures on an oscillating panel, see Ref. [2]. The simplest of these and consequently the most widely used is the so called " piston theory, see Ref. [3]. Once the mathematical model has been established, the methods of solution are required to investigate the parameters variations. Since an exact solution of the nonlinear flutter problem is not known, an approximate method is used. The most straight forward method used in the analysis for the flutter of a finite panel is the Galerkin method. It is used to reduce the mathematical problem to a system of nonlinear, ordinary, integral-differential equations in time see Ref. [4], which are solved by the method of describing functions /harmonic balance method or direct numerical integration. Fortunately, as far as the treatment of the panel flutter of a finite plate is concerned, Galrkin's method gives qualitatively correct results. Another more powerful method (in case of linear analysis) used to check the result of Galerkin's method is the Laplace transformation method see Ref. [5]. Another method for treating the nonlinear panel flutter problems is the so called perturbation technique, that is used to examine theoretically the general characteristics of non-linear flutter at high supersonic Mach number, see Ref. [6]. Von Karman's large deflection plate theory and the quasi-steady aerodynamic theory have been employed. The effect of structural damping has been included. Galerkin's technique has been used in the space variables and the ordinary differential system obtained is solved by an asymptotic expansion using method of multiple time scales. The results obtained show that, as a first approximation, the amplitude of the limit cycle depends only upon the fundamental parameter (non-dimensional aerodynamic loading), the aspect ratio, and the damping parameter (including structural damping effect). The

results are in excellent agreement with those obtained numerically in Ref. [7] and Ref. [8]. A comparison between theoretical and experimental results is required to modify or to improve the mathematical models if necessary. A comparative experimental and theoretical study of the flutter of flat panels in low supersonic flow was performed. The pre-flutter panel motion and the motion during flutter were studied in detail, as shown in Ref. [5]. A detailed comparison reveals considerable disagreement in the flutter boundaries at supersonic Mach number less than 1.4. The agreement between theory and experiment improves at the higher Mach numbers. In fact the disagreements between theory and experiment are mainly due to four factors, these factors are:

-The use of linear aerodynamic theory, where most of the theoretical investigations have utilized two-dimension static aerodynamic theory (both with and without damping), despite the fact that two dimensional theory is considered applicable only for a limited range of panel length-to-width ratio and Mach number.

- Neglecting boundary layer and aerodynamic heating effects (particularly panel excited by turbulence).

- The imprecise idealization of the complicated panel support conditions and cavity effects.

- Neglecting nonlinear mid-plane stresses and buckling is an over-idealization. Considering all of the above factors in formulating the mathematical model, the results of the theory and the experiment will be in excellent agreement, and thus the mathematical model can be used to investigate the variation in parameters. Flutter oscillations rarely cause immediate failure of the panel, but they may produce fatigue failure after a sufficient period of time. The need to prevent this occurrence, either by suppressing flutter entirely or by limiting the severity of the panel motion, often becomes the critical design criterion that determines the required thickness (or more generally the stiffness) of the panel. Many parameters govern the resonance fatigue behavior including the detail design, the skin thickness and materials, the stiffener configurations and the damping of the structure.

II. Problem Formulation

II.1. Equations of Motion

The plate under consideration is shown in Fig. 1.The dimensions and properties of the Plate are given in Table 2. The axes are taken to be such that the x-, y- axes are in the plane of the plate passing through its reference plane (z=0), while the z- axis is positive upwards. Under the assumptions that plate thickness is small in comparison with smallest lateral dimension, which is the case in most practical applications, the Kirchhoff's hypothesis may be assumed to be valid. With this assumption the in-plane displacements u, v and the transverse deflection w at an arbitrary point of the plate in the x, y, and z directions will be:

$$\left.\begin{aligned} u(x, y, z, t) &= u^{o}(x, y, z) - z\, w^{o}_{,x} \\ v(x, y, z, t) &= v^{o}(x, y, z) - z\, w^{o}_{,y} \\ w(x, y, z, t) &= w^{o}(x, y, t) \end{aligned}\right\} \quad (1)$$

where u^{o}, v^{o}, and w^{o} are the values of u, v, and w at the reference plane. It is considered here that the plate thickness is constant and the reference plane coincides with the midplane of the undeformed plate. The total plate strains using Kirchhoff's hypothesis of thin plates are:

$$\left.\begin{aligned} \varepsilon_x &= \varepsilon^{o}_x + z\kappa_x \\ \varepsilon_y &= \varepsilon^{o}_y + z\kappa_y \\ \varepsilon_{xy} &= \varepsilon^{o}_{xy} + z\kappa_{xy} \end{aligned}\right\} \quad (2)$$

where ε^{o}_x, ε^{o}_y, and ε^{o}_{xy} are the reference plane strains, while κ_x, κ_y, and κ_{xy} are the plate curvatures. They are given, according to Von Karman-type geometric nonlinearity, as:

mid-plane strain:

$$\left.\begin{aligned} \varepsilon^{o}_x &= u^{o}_{,x} + (1/2)\, w^{o}_{,x}{}^2 \\ \varepsilon^{o}_y &= v^{o}_{,y} + (1/2)\, w^{o}_{,y}{}^2 \\ \varepsilon^{o}_{xy} &= u^{o}_{,y} + v^{o}_{,x} + w^{o}_{,x}\, w^{o}_{,y} \end{aligned}\right\} \quad (3)$$

mid-plane curvature:

$$\left.\begin{aligned} \kappa_x &= -w_{,xx} \\ \kappa_y &= -w_{,yy} \\ \kappa_{xy} &= -2\, w_{,xy} \end{aligned}\right\} \quad (4)$$

Once the total strains are obtained, the stresses can be calculated from the stress-strain relations where:

$$\left.\begin{aligned}\sigma_x &= \frac{E}{1-\nu^2}(\varepsilon^o_x + \nu\,\varepsilon^o_y)\\ \sigma_y &= \frac{E}{1-\nu^2}(\varepsilon^o_y + \nu\,\varepsilon^o_x)\\ \sigma_{xy} &= \frac{E}{2(1+\nu)}(\varepsilon^o_{xy})\end{aligned}\right\} \qquad (5)$$

As in the classical plate theory, the stress resultants and couples are defined by:

$$[N_x, N_y, N_{xy}] = \int_{-h/2}^{h/2} [\sigma_x, \sigma_y, \sigma_{xy}]\, dz \qquad (6\text{-a})$$

$$[M_x, M_y, M_{xy}] = \int_{-h/2}^{h/2} [\sigma_x, \sigma_y, \sigma_{xy}]\, z dz \qquad (6\text{-b})$$

where:

N_x, N_y, N_{xy} are the membrane forces per unit length.

M_x, M_y, M_{xy} are the bending and twisting moments per unit length.

The equations of motion of the plate in terms of the plate displacements u, v, and w are obtained by substituting the calculated stress resultants and couples into the equations of equilibrium given by Ref. [10]:

$$N_{x,x} + N_{xy,y} = 0 \qquad (7\text{-a})$$

$$N_{xy,x} + N_{y,y} = 0 \qquad (7\text{-b})$$

$$M_{x,xx} + 2M_{xy,xy} + M_{y,yy} + N_x w_{,xx} + 2N_{xy} w_{,xy} + N_y w_{,yy} + q = \rho h w_{,tt} \qquad (7\text{-c})$$

Where, q stands for all external applied loads on the plate, like the aerodynamic loading, cavity pressure, and static differential pressure, etc. It is to be mentioned that the foregoing equations of motion for the plate were derived based on the assumption of Kirchhoff's hypothesis, that the effect of transverse shear deformation is neglected, (it is true that the thinner the plate the more accurate the hypothesis). Consequently the plate is considered as homogeneous, isotropic, and of span-to thickness ratio more than 15 satisfies all the requirements to use the previous assumptions.

II.2. Effect of Applied In-Plane Loading

If constant in-plane forces are applied in both the x-, and y- directions, the resultant stresses may be written as:

$$N_x^{(T)} = N_x \pm N_x^{(AL)} \qquad (8\text{-a})$$

$$N_y^{(T)} = N_y \pm N_y^{(AL)} \qquad (8\text{-b})$$

Where,

$N_x^{(T)}$ and $N_y^{(T)}$ are the total in-plane loading.

$N_x^{(AL)}$ and $N_y^{(AL)}$ are the applied tensile or compression in-plane loading.

The negative sign is for compression and may cause buckling, while the positive sign is for tension and has the effect to oppose the applied lateral loading.

II.3. Thermal Stresses in the Plate

If the plate is free to deform and if its temperature is raised uniformly up to a temperature T, above the stress-free temperature, the thermal strain induced at any point of the plate material will be:

$$\varepsilon_x = \alpha T \quad \text{and} \quad \varepsilon_y = \alpha T \qquad (9)$$

Where α is the coefficient of thermal expansion (assumed constant). The temperature T can be regarded as the temperature change relative to an arbitrary temperature that is uniform throughout the plate. If the plate is clamped all along its boundaries, the strains in the plane of the plate are zero and the stresses $\sigma_x^{(AL)}$ and $\sigma_y^{(AL)}$ will be given by:

$$\sigma_x^{(AT)} = \sigma_y^{(AT)} = \frac{-E\,\alpha\,T}{(1-\nu)} \qquad (10)$$

Consequently the induced in-plane loadings due to thermal stresses are:

$$N_x^{(AT)} = \int_{-h/2}^{h/2} \sigma_x^{(AT)}\, dz \qquad (11)$$

$$N_y^{(AT)} = \int_{-h/2}^{h/2} \sigma_y^{(AT)}\, dz \qquad (12)$$

and the total in-plane loading due to thermal stresses are:

$$N_x^{(T)} = N_x \pm N_x^{(AT)} \qquad (13\text{-a})$$

$$N_y^{(T)} = N_y \pm N_y^{(AT)} \qquad (13\text{-b})$$

It is clear that the negative sign indicates a destabilizing effect while the positive sign indicates stabilization as explained earlier.

II.4. Aerodynamic Loading

When an inviscid fluid with free stream velocity U_∞ flows past a two dimensional flexible plate in the longitudinal direction (x-direction) as shown in Fig. 1, with no static pressure differential across the plate, then the velocity potential $\Phi(x, y, z, t)$ may be described by its linearized form (from the momentum equation) as:

$$\nabla^2\Phi - \left(\frac{1}{\partial t} + U_\infty \frac{1}{\partial x}\right)^2 \Phi = 0 \qquad (14)$$

Where c, is the velocity of sound in the fluid. It is assumed that the supersonic flow over the plate is free of shocks, that is, the flow is irrotational. The boundary conditions on the velocity potential are:

$$\frac{\partial \Phi}{\partial z} = \begin{cases} \left(\frac{1}{\partial t} + U_\infty \frac{1}{\partial x}\right) w & \text{on the plate} \\ 0 & \text{off the plate} \end{cases} \qquad (15)$$

Where w is the plate lateral deflection. The pressure is given, from the unsteady Bernoulli's equation, by:

$$P = -\rho_\infty \left(\frac{1}{\partial t} + U_\infty \frac{1}{\partial x}\right) \Phi \qquad (16)$$

Where ρ_∞ is the free stream density.

Equations (14) and (16) subjected to the boundary conditions (15) can be solved by integral transformation, see Ref. [11], to obtain an expression for the pressure loading on the plate valid for all Mach numbers at which linearization is acceptable. One of the most acceptable expressions used to represent the aerodynamic loading is called the quasi-steady aerodynamic approximation, written as:

$$P = \frac{-2q}{\beta}\left\{\frac{\partial w}{\partial x} + \frac{\beta^2 - 1}{\beta^2}\,\frac{1}{U_\infty}\frac{\partial w}{\partial t}\right\} \qquad (17)$$

Where $\beta^2 = M^2 - 1$

The first term in equation (17) represents the aerodynamic loading on the plate while the second term represents aerodynamic damping. This expression, which is derived from the expansion of the reduced frequency of the exact two dimensional unsteady flow, can also be reduced to the well known piston theory see Ref. [3], which is applicable in the case of higher Mach numbers (M>2.0). It is given in the following form:

$$P = \frac{-2q}{\beta}\left\{\frac{\partial w}{\partial x} + \frac{1}{U_\infty}\,\frac{\partial w}{\partial t}\right\} \qquad (18)$$

It is clear from both expressions that the only difference is in the damping term. It is obvious that the difference is small for higher Mach numbers (especially if it is considered that aerodynamic damping effect is small). In this formulation, the aerodynamic load and the aerodynamic damping will be represented by the use of the quasi-steady aerodynamic approximation expression.

II.5. Cavity Aerodynamics

in formulating the problem we assume that the effect of the air beneath the plate can be neglected. This assumption can be considered as true when the depth of the cavity is large enough (large with respect to the plate spatial dimension). When, as quite often is the case, the cavity depth "d" is smaller than the smaller spatial dimensions, it is necessary to consider its effect. It is shown in Ref. [12], that the cavity has two main effects. First, the static pressure within the cavity may be different from that of the flow over the plate surface. This static pressure difference will act as to bend the plate and consequently create a tensile in-plane force throughout the mid-plane surface. Second, the plate motion may cause an increase in the cavity pressure which in turn changes the plate natural frequencies due to the spring action of the air in the cavity. The second effect will be represented with the help of the formulation given in Ref. [13]. In this formulation, the equation governing the acoustic effects of the cavity in case of non-viscous flow is represented as:

$$\nabla^2 \Phi - \frac{1}{c^2}\,\frac{\partial^2 \Phi}{\partial t^2} = 0 \qquad (19)$$

and the pressure due to the plate motion is given by:

$$P = -\rho_c \,\frac{\partial \Phi}{\partial t} \qquad (20)$$

Where ρ_c is the density of the fluid in the cavity.

The boundary condition on are given by:

$$\frac{\partial \Phi}{\partial z} = \frac{\partial w}{\partial t} \quad (\text{at } z=0) \qquad (21\text{-a})$$

$$\frac{\partial \Phi}{\partial z} = 0 \quad (\text{at } z=-d) \qquad (21\text{-b})$$

$$\frac{\partial \Phi}{\partial n} = 0 \quad (\text{on sides of the cavity}) \qquad (21\text{-c})$$

Equations (19) and (20) will be solved by the transformation method, subjected to the boundary conditions given by equation (21). After a series of substitutions, transformations, and integrations a final

expression is obtained which represents the equilibrium static pressure that would be obtained by computing the isentropic pressure rise due to the change in the cavity volume caused by the instantaneous plate deflection w. This equilibrium static pressure takes the form:

$$Pc = -\frac{\rho_c c^2}{abd}\int_0^1\int_0^1 w(x, y, t)\, dy\, dx \qquad (22)$$

II.6. Final form of the Equations

The final form of the aerodynamic equations after substituting the terms representing the external applied loads can be written as:

$$\frac{\partial}{\partial x}[N_x \pm N_x^{(AL)} \pm N_x^{(AT)}] + \frac{\partial}{\partial y}N_{xy} = 0 \qquad (23\text{-a})$$

$$\frac{\partial}{\partial y}[N_y \pm N_y^{(AL)} \pm N_y^{(AT)}] + \frac{\partial}{\partial x}N_{xy} = 0 \qquad (23\text{-b})$$

$$M_{x,xx} + 2M_{xy,xy} + M_{y,yy} + N_x w_{,xx} + N_{xy} w_{,xy} + N_y w_{,yy} \pm [N_x^{(AL)} + N_x^{(AT)}] w_{,xx} \pm [N_y^{(AL)} + N_y^{(AT)}] w_{,yy} - \frac{2q}{\beta}\left\{\frac{\partial w}{\partial x} + \frac{1}{U_\infty}\frac{\beta^2-1}{\beta^2}\frac{\partial w}{\partial t}\right\} - \frac{\rho_c c^2}{abd}\int_0^a\int_0^b w(x, y, t)dydx - \rho_p h_p w_{,tt} = 0 \qquad (23\text{-c})$$

The applied in-plane loadings are uniform and constant throughout the plate so that the first two equations will be written as:

$$N_{x,x} + N_{xy,y} = 0$$
$$N_{xy,x} + N_{y,y} = 0 \qquad (24)$$

Substituting for N_x, N_y, N_{xy}, M_x, M_y, and M_{xy} from equations (6) into equations (24), (23-c) to get the equations of the plate in terms of the displacements u, v, and w, which represents the set of nonlinear partial differential equations of motion of the plate. It is common and preferable to put these equations into a non-dimensional form by introducing the following non-dimensional parameters:

$$\bar{u} = \frac{u}{h} \qquad \bar{v} = \frac{v}{h} \qquad \bar{w} = \frac{w}{h}$$

$$\bar{\xi} = \frac{x}{a} \qquad \bar{\eta} = \frac{y}{b} \qquad f = \frac{a}{b}$$

$$\frac{\partial}{\partial x} = \frac{1}{a}\frac{\partial}{\partial \xi} \qquad \frac{\partial}{\partial y} = \frac{1}{b}\frac{\partial}{\partial \eta}$$

and $\tau = \omega_r . t$ where $\omega_r = \frac{D\pi^4}{\rho_p h_p a^4}$

After a series of substitutions and simplifications the following non-dimensional form of the plate aero-elastic equations is obtained.

The U-equation is given as:

$$\bar{u}_{,\xi\xi} + d_1 f^2 \bar{u}_{,\eta\eta} + d_2 f \bar{v}_{,\xi\eta} + \frac{h}{a}\{\bar{w}_{,\xi}\bar{w}_{,\xi\xi} + d_1 f^2 \bar{w}_{,\xi}\bar{w}_{,\eta\eta} + d_2 f^2 \bar{w}_{,\eta}\bar{w}_{,\xi\eta}\} = 0 \qquad (25\text{-a})$$

The V-equation is given as:

$$d_1 \bar{v}_{,\xi\xi} + f^2 \bar{v}_{,\eta\eta} + d_2 f \bar{u}_{,\xi\eta} + \frac{h}{b}\{f^2 \bar{w}_{,\eta}\bar{w}_{,\eta\eta} + d_1 \bar{w}_{,\eta}\bar{w}_{,\xi\xi} + d_2 \bar{w}_{,\xi}\bar{w}_{,\xi\eta}\} = 0 \qquad (25\text{-b})$$

The W-equation is given as:

$$\frac{1}{\pi^4}\{\bar{w}_{,\xi\xi\xi\xi} + 2f^2\bar{w}_{,\xi\xi\eta\eta} + f^4\bar{w}_{,\eta\eta\eta\eta}\} \pm \{\bar{n}_\eta^{(AL)} + \bar{n}_\eta^{(AT)}\} \pm \{\bar{n}_\xi^{(AL)} + \bar{n}_\xi^{(AT)}\} + \lambda_a\bar{w}_{,\xi} + \lambda_d\bar{w}_{,\tau} + \lambda_c\int_0^1\int_0^1 w d\eta d\xi + w_{,\tau\tau} - \frac{1}{\pi^4}\{12\frac{a}{h}[\bar{u}_{,\xi}\bar{w}_{,\xi\xi} + \nu f^2\bar{u}_{,\xi}\bar{w}_{,\eta\eta} + (-\nu) f^2\bar{u}_{,\eta}\bar{w}_{,\xi\eta} + f^3\bar{v}_{,\eta}\bar{w}_{,\eta\eta} + \nu f\bar{v}_{,\eta}\bar{w}_{,\xi\xi} + (1-\nu) f\bar{v}_{,\xi}\bar{w}_{,\xi\eta}] + 6[\bar{w}^2_{,\xi}\bar{w}_{,\xi\xi} + f^4\bar{w}^2_{,\eta}\bar{w}_{,\eta\eta} + f^2\bar{w}^2_{,\xi}\bar{w}_{,\eta\eta} + f^2\bar{w}^2_{,\eta}\bar{w}_{,\xi\xi} + f^2\bar{w}_{,\xi}\bar{w}_{,\eta}\bar{w}_{,\xi\eta}]\} = 0 \qquad (25\text{-c})$$

Where $d_1 = (1-\nu)/2$ and $d_2 = (1+\nu)/2$

Equations (25-a), (25-b), and (25-c) represent the final form of the plate equations of motion in a non-dimensional form. The form of these equations is general see Ref [1] and Ref. [14]. The assumptions made in the previous formulations are based on thin plate theory and for plates under large deflections, the middle plane strain must be considered. The applied lateral loads considered are those due to aerodynamic loading and cavity effect. These loads represent the coupling between the elasticity parts of the problem with the aerodynamic parts due to flow over the plate and cavity beneath it. The nonlinear part of the problem

represents the membrane forces induced due to large plate deflection. This term limits the amplitude of the fluttering motion of the plate. Other terms corresponding to in-plane loading will have either stabilizing or destabilizing effects depending on their signs in the equation. Finally, the damping had been represented by the coefficient of $w_{,\tau}$. This coefficient represents the aerodynamic damping and can also include the structural damping of the plate.

III. Flutter Analysis

Galerkin's method is used to reduce the obtained equations of motion to a set of nonlinear ordinary differential equations having the non-dimensional time variable as an independent variable. The displacement u, v, and the deflection w are expanded in the form of a generalized double series of modes. These modes satisfy the appropriate geometric boundary conditions of the plate. The assumed displacement solution may be taken as:

$$\bar{u}^{o}(\xi,\eta,\tau)=\sum_{m=1}^{\infty}\sum_{n=1}^{\infty}\bar{U}_{mn}(\tau)\bar{X}^{(u)}{}_{m}(\xi)\bar{Y}^{(u)}{}_{n}(\eta) \quad (26\text{-a})$$

$$\bar{v}^{o}(\xi,\eta,\tau)=\sum_{m=1}^{\infty}\sum_{n=1}^{\infty}\bar{V}_{mn}(\tau)\bar{X}^{(v)}{}_{m}(\xi)\bar{Y}^{(v)}{}_{n}(\eta) \quad (26\text{-b})$$

$$\bar{w}^{o}(\xi,\eta,\tau)=\sum_{m=1}^{\infty}\sum_{n=1}^{\infty}\bar{W}_{mn}(\tau)\bar{X}^{(w)}{}_{m}(\xi)\bar{Y}^{(w)}{}_{n}(\eta) \quad (26\text{-c})$$

in which $\bar{X}(\xi)$ and $\bar{Y}(\eta)$ are the modal functions that satisfy the boundary conditions imposed on $\bar{u}$, $\bar{v}$, or $\bar{w}$ in the ξ and η direction respectively. It is also necessary that these modal functions constitute a complete set of functions over the plate $0 \le \xi, \eta \le 1$ so that any continuous functions $\bar{u}$, $\bar{v}$, or $\bar{w}$ satisfying the geometric boundary conditions of the plate can be approximated uniformly by an expression of the form given above. The series (26-a, b, c) for u, v, and w are substituted into the equations of motions (25-a, b, c), and the resulting expressions are multiplied successively by the corresponding modal functions and then integrating over the surface of the plate. The modal equations obtained in this manner after manipulating appear in the following tensorial form:

$$A1^{mn}_{ij}\bar{U}_{mn}+A2^{mn}_{ij}\bar{V}_{mn}+A3^{mnrs}_{ij}\bar{W}_{mn}\bar{W}_{rs}=0 \quad (27\text{-a})$$

$$B1^{mn}_{ij}\bar{V}_{mn}+B2^{mn}_{ij}\bar{U}_{mn}+B3^{mnrs}_{ij}\bar{W}_{mn}\bar{W}_{rs}=0 \quad (27\text{-b})$$

$$C1^{mn}_{ij}\bar{W}_{mn,\tau\tau}+\lambda_d C1^{mn}_{ij}\bar{W}_{mn,\tau}+\lambda_a C2^{mn}_{ij}\bar{W}_{mn}+\lambda_c C3^{mn}_{ij}\bar{W}_{mn}+$$
$$C4^{mn}_{ij}\bar{W}_{mn}\pm\{n_\xi^{(AL)}+n_\xi^{(AT)}\}C5^{mn}_{ij}\bar{W}_{mn}\pm\{n_\eta^{(AL)}+$$
$$n_\eta^{(AT)}\}C6^{mn}_{ij}\bar{W}_{mn}+C7^{mnlp}_{ij}\bar{U}_{mn}\bar{W}_{lp}+$$
$$C8^{mnlp}_{ij}\bar{V}_{mn}\bar{W}_{lp}+C9^{mnlprs}_{ij}\bar{W}_{mn}\bar{W}_{lp}\bar{W}_{rs}=0 \quad (27\text{-c})$$

The vectors $\bar{U}(\tau)$ and $\bar{V}(\tau)$ are computed from equations (27-a) and (27-b) algebraically and then substituted pinto equation (27-c) to yield the Duffing-type equation in the following form:

$$C1^{mn}_{ij}\bar{W}_{mn,\tau\tau}+\lambda_d C2^{mn}_{ij}\bar{W}_{mn,\tau}+C3^{mn}_{ij}\bar{W}_{mn}\pm\{n_\xi^{(AL)}+$$
$$n_\xi^{(AT)}\}C4^{mn}_{ij}\bar{W}_{mn}\pm\{n_\eta^{(AL)}+n_\eta^{(AT)}\}C5^{mn}_{ij}\bar{W}_{mn}+$$
$$\lambda_a C6^{mn}_{ij}\bar{W}_{mn}+\lambda_c C7^{mn}_{ij}\bar{W}_{mn}+T^{mnlprs}_{ij}\bar{W}_{mn}\bar{W}_{lp}\bar{W}_{rs}=0 \quad (28)$$

This tensorial nonlinear ordinary differential equation represents a set of (ixj) nonlinear ordinary differential equation which can not be solved exactly.

III.1 Displacement Functions and Boundary Conditions

The procedure presented above is general and can be applied for any thin flat rectangular plate with various boundary conditions. To complete the solution, the boundary conditions for the plate must be specified. For the purpose of comparison with the result obtained by the experimental reports, see Ref. [15], the boundary conditions are specified to be clamped all around with no in-plane movements, so that the out of plane boundary condition is fully-clamped and the in-plane

boundary condition is edge-fixed, and these conditions are written as:

$w = w_{,\xi} = u^o = v^o = 0$
at both x=0 and x=1 (29-a)

$w = w_{,\eta} = u^o = v^o = 0$
at both y = 0 and y = 1 (29-b)

And the modal functions are given by:

$$X^{(u)}_m(\xi) = X^{(v)}_m(\xi) = \sin(m\pi\xi) \quad (30\text{-a})$$
$$Y^{(u)}_n(\eta) = Y^{(v)}_n(\eta) = \sin(n\pi\eta) \quad (30\text{-b})$$

While: $X^{(w)}_m(\xi)=\cosh\alpha_m\xi-\cos\alpha_m\xi-\gamma_m(\sinh\alpha_m\xi-\sin\alpha_m\xi)$ (30-c)

and: $Y^{(w)}_n(\eta)=\cosh\alpha_n\eta-\cos\alpha_n\eta-\gamma_n(\sinh\alpha_n\eta-\sin\alpha_n\eta)$ (30-d)

where α_m and γ_m are the coefficients for the m^{th} flexural mode and can be calculated from the following equation:

$$\cosh\alpha_m\cos\alpha_m = 1 \quad (31\text{-a})$$
$$\cosh\alpha_m-\cos\alpha_m\xi-\gamma_m(\sinh\alpha_m-\sin\alpha_m)=0 \quad (31\text{-b})$$

The values of these coefficients are given in Table 1. see also Ref. [16]. Once the displacement modal functions are specified for the prescribed boundary conditions, the coefficients of integration represented by the matrices A1 to A3, B1 to B3, C1 to C9, and T can be calculated numerically. The number of the terms in the assumed displacement series solution given by (26-a), (26-b), and (26-c) are arbitrary. As the number of terms increases the obtained results will be more accurate. The limiting factor in this process is the computer time (cpu time), which increases dramatically as the number of terms in the series increases.

III.2 Harmonic Balance Method

Since an exact solution of equation (28) is not available, an approximate solution will be obtained by the method of harmonic balance. This method is used to seek a periodic solution. The existence of such solution indicates the occurrence of self-excited vibrations of the limit-cycle type. The method also yields the characteristics of the vibrations such as the frequency, amplitudes and phase angles, and it can be used to study the effect of parameters on plate behavior. In the frequency domain the differential operator d/dT is replaced by $j\omega$ and, consequently, the system of nonlinear differential equations is converted to a set of nonlinear algebraic equations. When this set has a solution with real positive values of frequency and amplitude and real values of the phase angles, it indicates the occurrence of limit-cycle oscillations of the specified form. Since the experimental results, see Ref. [4], [15], [22], and [24] show the response of the plate under consideration during flutter to be oscillating harmonically at its fundamental frequency, one seeks a solution of the following form:

$$W_{mn}(\tau) = A_{mn}\sin(\omega\tau + \Phi_{mn}) \quad (32\text{ a})$$

Where Φ_{11} is considered to be zero. Consequently:

$$\overline{W}_{mn}=A_{mn}[\cos\Phi_{mn}+j\sin\Phi_{mn}]\sin\omega_\tau \quad (32\text{-b})$$
$$\overline{W}_{mn,\tau}=\omega A_{mn}[j\cos\Phi_{mn}-\sin\Phi_{mn}]\sin\omega_\tau \quad (32\text{-c})$$
$$\overline{W}_{mn,\tau\tau}=-\omega^2 A_{mn}[\cos\Phi_{mn}+j\sin\Phi_{mn}]\sin\omega_\tau \quad (32\text{-d})$$
$$\overline{W}_{mn}\overline{W}_{rs}\overline{W}_{pq}=A_{mn}A_{rs}A_{pq}\{[\cos\Phi_{mn}\cos\Phi_{rs}\cos\Phi_{pq}\sin\Phi_{mn}\sin\Phi_{rs}\cos\Phi_{pq}\cos\Phi_{mn}\sin\Phi_{rs}\sin\Phi_{pq}-\sin\Phi_{mn}\cos\Phi_{rs}\sin\Phi_{pq}]-j[\sin\Phi_{mn}\sin\Phi_{rs}\sin\Phi_{pq}-\cos\Phi_{mn}\cos\Phi_{rs}\sin\Phi_{pq}\sin\Phi_{mn}\cos\Phi_{rs}\cos\Phi_{pq}\cos\Phi_{mn}\sin\Phi_{rs}\cos\Phi_{pq}]\}\sin^3\omega_\tau \quad (32\text{-e})$$

Where, $\sin^3\omega_\tau=\frac{1}{4}(3\sin\omega_\tau+\frac{3}{4}\sin3\omega_\tau)$ (32-f)

The second term which is of higher harmonic will be dropped out and:

$$\sin^3\omega_\tau = \frac{3}{4}\sin\omega_\tau \quad (32\text{-g})$$

Substituting $\overline{W}_{mn}$ from equations (32) into the Duffing type equation and equating separately the real and imaginary parts of the equations, the set of 2(ixj) nonlinear algebraic equations in the unknown variables given by (ixj) amplitudes, ((ixj)-1) phase angles, and the flutter frequency (ω_f) is obtained. These equations are solved numerically by the modified Newton- Raphson algorithm.

III.3 Nonlinear Flutter Analysis

Flutter analysis is carried out with a three terms (m=3) in the stream-wise (x-direction) and three terms (n=3) in

the cross stream (y-direction) for the assumed series solution which will be sufficient for the convergence with acceptable accuracy and cpu time, see Ref. [21]. In fact for plates with high aspect ratios, the more terms in the stream-wise direction the more accurate will be the solution, see also Ref. [17] and [18].

The dimensions and material properties of the plate considered are shown in Table 2. The flutter analysis is started by specifying the flight conditions (the Mach number "M" and altitude of flight), the cavity parameter (volume beneath the plate) represented by the nondimensional parameter λ_c, and determining plate nondimensional lateral deflection $\overline{W}$ vs. the nondimensional aerodynamic loading λ_a. These procedures can be repeated for different parameters variation to investigate their effects on the plate behavior during flutter.

III.3.1 Determination of flutter boundary

The flutter onset condition is determined experimentally by Ref. [15], [22], and [24], as function of M, q, N_x, N_y, and the secondary parameters. Since N_x was a primary variable and had a strong influence on flutter, the boundary could be approached by increasing either N_x and N_y or q while holding the remaining parameters fixed. It is also found that the transition from stability to instability (flutter) may be best described as a change from random to periodic motion accompanied by a substantial increase in the strain amplitude. It is noticed that there is a gradual increase in the strain amplitude as dynamic pressure is increased from 200 to 600 psf. The strain amplitude increase is roughly in proportion to dynamic pressure and is caused by increasing wall turbulence in the tunnel. When the aerodynamic pressure, q, reached 650 psf, the strain increased sharply, indicating that the panel has become aeroelastically unstable. As q changed from 500 to 600 psf the output shows the emergence of a dominant frequency component and also begins to exhibit a beating characteristic. Just above the flutter boundary, the randomness disappears and the wave becomes periodic.

A comparison between the results obtained by the present work and those obtained by Ref. [15], [22], and [24], for the peak-to-peak panel displacement vs the dynamic pressure at the middle portion of the panel is shown in Fig. 2. In this comparison the plate material and dimensions are the same, while the Mach number, M, is different. The reason is that the Mach number used in the experimental results is ($1.1<M<1.4$), which cannot be used by the linearized quasi-steady aerodynamic theory, since it is applicable only for Mach number ($M>1.6$). The behavior of both the experimental and theoretical results is nearly the same, especially in the fluttering region. The difference in the critical flutter points in each of the previous comparisons, where the critical aerodynamic pressure, q_{cr}, from experiment is lower than that from theoretical solution, is due to the lower Mach number and the imprecise clamped boundary conditions attained in the experimental procedures.

III.3.2 Effect of plate thickness

It is known that one possible way to prevent flutter is to increase the plate rigidity by increasing its elasticity modulus or thickness. In Fig. 3 the nondimensional amplitude vs dynamic pressure for different thicknesses of the plate are shown. It is clear from the plot that as thickness increases, the critical value of the dynamic pressure, λ_c, increases. Another result is shown in Fig. 4, for the variation of the nondimensional amplitude vs the change of thickness of the plate. From these two plots it is clear that by increasing the plate thickness it is possible to prevent flutter by increasing the aerodynamic loading critical value

to higher values far from that at which the plate will operate.

III.3.3 Effect of cavity

The air within the cavity affects the flutter behavior of the plate. It has two separate effects on the panel modes and frequencies. The first effect is due to the compressibility of the air which acts as a spring and stiffens the plate. The second effect is that the cavity pressure increment due to the plate motion may cause an appreciable change in the natural frequencies of the plate. The change in the frequencies may consequently alter the stability boundaries of the plate. This effect is largest for the fundamental mode and less for the higher symmetrical modes. The second effect is due to the air acting as additional mass which tends to lower the panel frequencies in all modes. In some experimental work by Ref. [9], it is noted that the result for the two cases (with and without cavity) differ significantly, that the fundamental mode frequency was raised to such an extent as to be difficult to be located. Fig. 5 shows the change of the flutter frequency vs the change in the cavity depth. It clear that as the depth of the cavity decreases the frequency is increased. Fig. 6, shows the change in frequency ratio, ω_f/ω_o, vs the change in the cavity depths for different density ratio, ρ_c/ρ_∞. It is noted from this figure that the change is sharply decreasing in the region (I) of small cavity depths and starts to be negligible for higher cavity depths in region (II).

III.3.4 Effect of aspect ratio

This section is to investigate the effect of aspect ratio on the behavior of the plate in the fluttering region. Different aspect ratio ($3<f<5$) are considered. In Fig. 7, is shown the non-dimensional amplitude w vs the non-dimensional aerodynamic pressure λ_a for different aspect ratios. It is clear from the plot that as the aspect ratio increases the critical aerodynamic pressure will increase while the limit cycle amplitude will decrease. In Fig. 8, is shown the change in the three dominant modes (as shown in Fig. 9, Fig. 10, and Fig. 11)at a specific value of aerodynamic pressure in the flutter region vs the change in aspect ratio. The sharp changes in the modes at certain aspect ratios about (2.75) and also (6.5) are predictable. It is clear from Fig. 7. and Fig. 8, that as the aspect ratio is decreased or increased the critical aerodynamic loading is also decreased or increased as a consequence, and because in Fig. 8, the aerodynamic loading is fixed at the value (q_a = 300 psf), the sharp changes are due to the change from the flutter regime to the pre-flutter regime. In fact, it is noted that during flutter the dominant mode for the plate under consideration (f = 4.75) is the mode (2,1) as shown in Fig. 10, while the dominant mode for the same plate in the pre-flutter regime is the mode (1,1) as shown in Fig. 9. It is to be concluded that when flutter begins, a mode interchange occurs, and this was investigated experimentally by Ref. [15], [22], and [24], at the transition from stability to instability (flutter). In fact it is not necessary that the mode (2,1) to be the dominant mode for all aspect ratios, where for example in case of square plate mode (1,1) is the dominant one during flutter. Consequently, care must be taken when initializing the initial guess for solving the nonlinear algebraic equations.

III.3.4 Effect of damping

Two types of damping are considered in the previous formulations and are included in the total non-dimensional damping parameter λ_{td}. The first is the aerodynamic damping λ_{ad}, and the second is the structural damping λ_{sd}, given by:

$$\lambda_{ad} = \frac{2qa^4}{\beta D \pi^4} \frac{\beta^2-1}{\beta^2} \omega_r \qquad (33\text{-a})$$

$$\lambda_{ad} = \frac{G_s a^4}{D \pi^4} \omega_r \qquad (33\text{-b})$$

where, $G_s = g_n \omega_n \rho_p h_p$

is assumed constant structural damping for the n^{th} mode.

and, $g_n = 2\xi_n \frac{\omega}{\omega_n} = 2\xi_1 \frac{\omega}{\omega_n}$

is the equivalent structural damping and ξ_n is the critical damping ratio of any mode with frequency ω_n. Since, during flutter, ω_n is constant for all modes and in this analysis it is assumed that damping coefficient g_n for any mode ω_n is related to that of the fundamental mode ω_1 by the relation given above, we will assume that $g_n = g_1 = 0.03$, which is commonly used in flutter analysis see Ref. [19] and [26].

It is a well known fact that structural damping can significantly modify panel flutter boundaries. It always has a stabilizing effect on a fluttering plate. Fig. 12, shows the limit cycle amplitude vs the dynamic pressure for different values of the structural damping λ_{sd}. Also Fig. 13, shows the effect of the aerodynamic damping λ_{ad} on the limit cycle amplitude vs dynamic pressure see Ref. [23]. From the two Figures, it is clear that both types of damping can enhance the behavior of the plate during flutter. It is also obvious that the structural damping has a greater influence than the aerodynamic damping.

III.4 Linear Flutter Analysis

In linear analysis the problem of panel flutter is an eigenvalue problem in which the eigenvalues are obtained for a given value of the non-dimensional aerodynamic pressure λ_a. It is to be noted that in linear analysis the cpu time reduces dramatically so more (up to six) terms can be taken in both x- and y-directions. Fig. 14, shows that with the increase in the value of λ_a, the two natural frequencies coalesce to the critical eigen-value (ω_f) at a value of ($\lambda_a = \lambda_{a\ cr}$) and then becomes a complex conjugate pair for any value of $\lambda_a > \lambda_{a\ cr}$, see Ref. [20]. Hence, the stability criteria adopted here is that the critical non-dimensional dynamic pressure $\lambda_{a\ cr}$ is considered to be the lowest value of λ_a at which coalescence occurs among all values of limit cycle amplitudes corresponding to the linear case. In the absence of the aerodynamic damping, the flutter boundary corresponds to $\lambda_{a\ cr}$. When the aerodynamic damping is considered, the value of $\lambda_{a\ cr}$ increases, and the extent of its increase is calculated from the panel response parameters. For $\lambda_a < \lambda_{a\ cr}$, any disturbance to the panel decays, and the amplitude tends to zero, while for $\lambda_a > \lambda_{a\ cr}$, a limit cycle oscillation exists, and the amplitude increases as λ_a increases. As the aerodynamic pressure increases beyond flutter onset, the fundamental flutter frequency (or limit cycle frequency) also increases. It is to be noted also that the experimental flutter frequency is less than that calculated theoretically. For example, the flutter frequency obtained experimentally by Ref [15] and [30], is 145 Hz while the calculated one is 173 Hz for the same plate material and geometry and for the same conditions of loading. Actually the plate in experiment is clamped to a frame shown in Fig. 15, which is elastic and in this case the plate is elastically supported. The boundary conditions in this case are such that uniform rotational restrains on opposite edges are provided by a restoring moment which is proportional to the edge angle of rotation, while the transverse deflection on all edges is zero. The boundary conditions are:

$$\left.\begin{aligned}
&\frac{\partial^2 w}{\partial \xi^2} - k_{r\xi}\frac{\partial^2 w}{\partial \xi^2} = 0 \text{ and } w=0 \text{ at } \xi=-1/2\\
&\frac{\partial^2 w}{\partial \xi^2} + k_{r\xi}\frac{\partial^2 w}{\partial \xi^2} = 0 \text{ and } w=0 \text{ at } \xi=+1/2\\
&\frac{\partial^2 w}{\partial \eta^2} - k_{r\eta}\frac{\partial^2 w}{\partial \eta^2} = 0 \text{ and } w=0 \text{ at } \eta=-1/2\\
&\frac{\partial^2 w}{\partial \eta^2} + k_{r\eta}\frac{\partial^2 w}{\partial \eta^2} = 0 \text{ and } w=0 \text{ at } \eta=+1/2
\end{aligned}\right\} \quad (34)$$

Where $k_{r\xi}$ and $k_{r\eta}$ are the spring constants of the rotational springs on the boundaries $\xi = +1/2$ and $\xi = -1/2$ and $\eta = +1/2$ and $\eta = -1/2$, respectively. In linear analysis this problem is solved by assuming beam eigen-function in the η-direction and then solving the differential equation exactly to get

symmetric frequency equations. Then, by choosing approximate values for the spring constants we can determine the natural frequencies of the plate. The first eight natural frequencies of the plate are calculated and shown in Table 3, for the cases:

- Clamped all around.
- Simply supported all around.
- Elastically supported all around.
- Experimental results.

Although we get exactly the same values of the natural frequency of the plate as those from the experiment, it is tedious to consider the case of elastically supported boundary conditions for a nonlinear analysis.

IV. Conclusion

The following conclusive statements can be summarized based on the investigations and results obtained.

- For thin plates, where the deflection is at least of the same order of magnitude as the plate thickness, the nonlinear thin plate theory must be used. The nonlinearity, represented by the plate in-plane (membrane) forces created due to large deflection, is the main source that causes the amplitude of the plate deflection during flutter to be limited (limit cycle oscillation).
- The accuracy of the result depends on the number of terms in the assumed series solution. For plates with high aspect ratio and when the direction of the flow is parallel to the longitudinal direction, the more terms in that direction, the more accurate the obtained results. It is found that using three terms in both directions gives good agreements with the experimental results.
- In case of linear analysis, where formulation is more condensed and cpu time decreases dramatically, more terms can be taken in both directions for more accurate results. In fact, linear analysis may be used for rough estimation of the flutter point. It is also used to account for the complicated support conditions, which is tedious to handle in nonlinear analysis.
- The effect of different parameters (like cavity pressure, structural and aerodynamic damping, plate thickness, and in-plane loading) on flutter point were studied separately. There is good agreement, between the results for these variations obtained here and other existing results in the field of flutter analysis. The most important parameters, that have great influence on the onset of flutter, are found to be the plate thickness, the in-plane loading, and the structural damping.

LITERATURE CITED

[1] Bisplinghoff. R. L., Ashley, H., and Halfman, L. R. (1962). Aeroelasticity, Addison-Wesley Publishing Company, Inc.

[2] Dowell, E. H. (1975), Aeroelasticity of Plates and Shells, Noordhoff Int'l Publishing, pp. 51-70.

[3] Ashley, H. and Zartarian, G. (1956), "Piston Theory – A New Aerodynamic Tool for the Aeroelastician", Journal of Aeronautical Sciences, Vol. 23, pp. 1109-1118.

[4] Fung, Y. C. (1958), " On Two-Dimensional Panel Flutter", Journal of Aeronautical Sciences, Vol. 25, pp. 145-160.

[5] Goland, M. and Luke Y. L. (1954), "An Exact Solution for Two-Dimensional Linear Panel Flutter at Supersonic Speed", Journal of Aeronautical Sciences, 21, 4, pp 275-276.

[6] Morino, L. (1969), "A Perturbation Method for Treating Nonlinear Panel Flutter Problems", AIAA Journal, Vol. 7, No. 3, pp. 405-411.

[7] Dowell, E. H. and Voss, H. M. (1965), " Theoretical and Experimental Panel Flutter Studies in the Mach Number Range 1.0 to 5.0", AIAA Journal, Vol. 3, No. 12, pp. 2292-2304.

[8] Kobayashi, S. (1962), "Two Dimensional Panel Flutter I. Simply Supported Panel", Transactions of the Japan Society of Aeronautics and Space Science, Vol. 5, No. 8, pp. 90-102.

[9] Dowell, E. H. (1966), "Nonlinear Oscillations of a Fluttering Plate. I", AIAA Journal, Vol. 4, No. 7, pp. 1267-1275.

[10] Chia, C. Y. (1980), Nonlinear Analysis of Plates, McGraw Hill Int'l Book Company.

[11] Dowell, E. H. (1971), "Generalized Aerodynamic Forces on a Flexible Plate Undergoing Transient Motion in a Shear Flow with an Application to Panel Flutter", AIAA Journal, Vol. 9, No. 5, pp. 834-841.

[12] Dowell, E. H. and Voss, H. M. (1963), "The Effect of a Cavity on Panel Vibration", AIAA Journal, Vol. 1, No. 2, pp. 476-477.

[13] Dowell, E. H. (1970), "Panel Flutter: A Review of the Aeroelastic Stability of Plates and Shells", AIAA Journal, Vol. 8, No. 3, pp. 385-399.

[14] Timoshenko, S. and Woinowsky-Krieger, S. (1959), Theory of Plates and Shells, McGraw-Hill Book Company, Inc., N.Y.

[15] Kappus, H. P., Lemley, C. E., and Zimmerman, N. H. (1971), "An Experimental Investigation of High Amplitude Panel Flutter", National Aeronautics and Space Administration. (NACA CR- 1837) Washington, D. C. May 1971.

[16] Young, D. (1950), "Vibration of Rectangular Plates by the Ritz Method", Journal of Applied Mechanics, Paper No. 50-APM-18, pp. 448-453.

[17] Dowell, E. H. and Ventres, C. S. (1970), "Flutter of Low Aspect Ratio Plates" AIAA Journal, Vol. 8, No. 6, pp. 1162-1164.

[18] Kobayashi, S. (1962), "Two Dimensional Panel Flutter II. Clamped Panel", Transactions of the Japan Society of Aeronautics and Space Science, Vol. 5, No. 8, pp. 102-118.

[19] Dugundji, J. (1966), "Theoretical Consideration of Panel Flutter at High Supersonic Mach Number", AIAA Journal, Vol. 4, No. 7, pp. 1257- 1266.

[20] Abou-Amer S. 1991. "Control of Panel Flutter at High Supersonic Speed", submitted in partial fulfillment of requirements for the degree of doctor of philosophy in Mechanical and Aerospace Engineering in the Graduate School of the Illinois Institute of Technology. Chicago, Illinois.

[21] Dowell, E. H. (1967), "Nonlinear Oscillations of a Fluttering Plate. II", AIAA Journal, Vol. 5, No. 10, pp. 1856-1862.

[22] Dowell, E. H. (1968), "Theoretical-Experimental Correlation of Plate Flutter Boundaries at Low Supersonic Speeds", AIAA Journal, Vol. 6, No. 9, pp. 1810-1811.

[23] Dowell, E. H. (1973), "Aerodynamic Boundary Effect on Flutter and Damping of Plate", J. AIRCRAFT, Vol. 10, No. 1, pp. 734-738.

[24] Lock, M. H. and Fung, Y. C. (1961), "Comparative Experimental and Theoretical Studies of Flutter of Flat Panels in a Low Supersonic Flow", AFOSR TN 670, Guggenheim Aero. Lab., Calif. Inst. Tech., Pasadena, Calif.

[25] Ventres, C. S. and Dowell E. H. (1970), "Comparison of Theory and Experiment of Nonlinear Flutter of Loaded Plates", AIAA Journal, Vol. 8, No. 1, pp. 2022-2030.

[26] Voss, H. M. and Dowell, E. H. (1964), "Effect of Aerodynamic Damping on Flutter of Thin Panels", AIAA Journal, Vol. 2, No. 1, pp. 119-120.

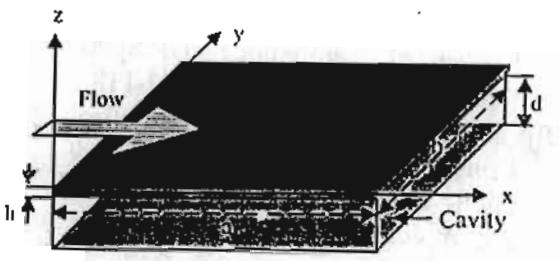

Fig. 1, Geometry of the Plate with Axes System

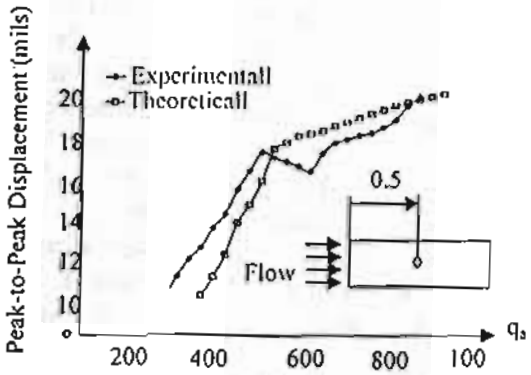

Fig. 2, Peak-to-Peak Displacement vs. Dynamic Pressure at the Center of the Plate, Comparison with the Experimental Result.

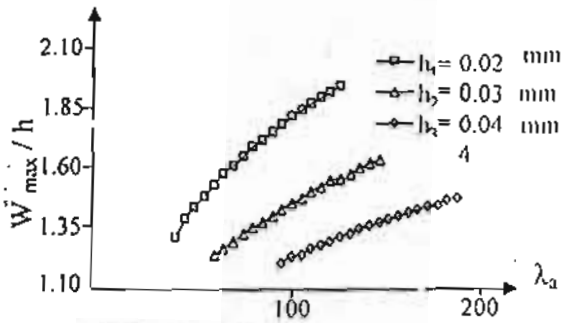

Fig. 3, Limit Cycle Amplitude vs. Dynamic Pressure for Three Plates of the Same Material and Different Thicknesses.

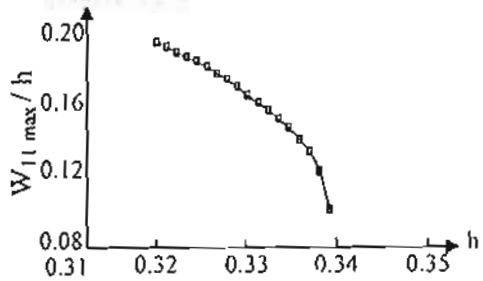

Fig. 4, Nondimensional Maximum Deflection Mode (1, 1) vs. Plate Thickness Change

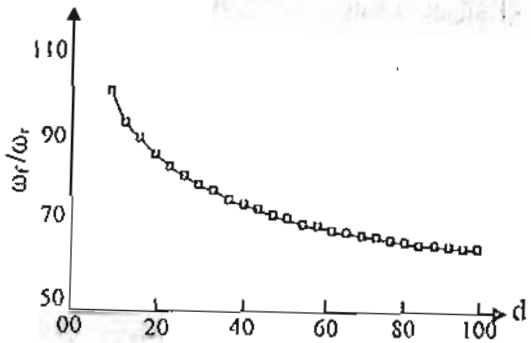

Fig. 5, Change in Flutter Frequency Ratio vs. Cavity Depth (d).

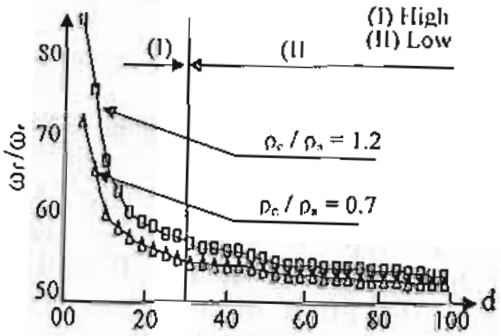

Fig. 6, The Change of the Frequency Ratio with the Change of Cavity

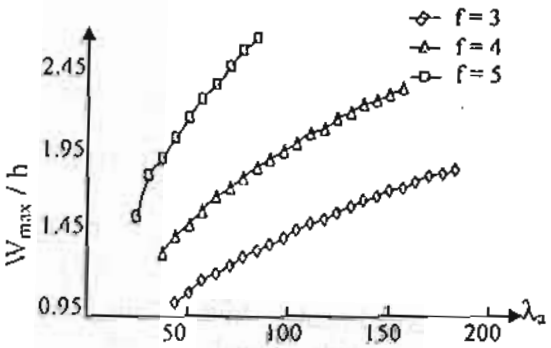

Fig. 7, Limit Cycle Amplitude vs. Dynamic Pressure for Different Aspect Ratios

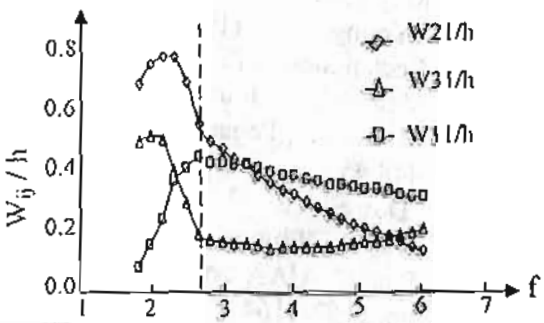

Fig. 8, Three Dominant Modes vs. Aspect Ratio for q_a =300 psf

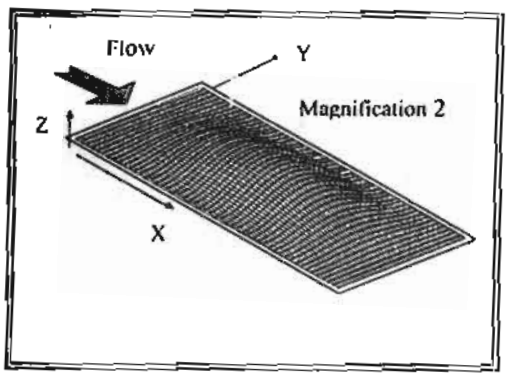

Fig. 9, Deflection of the Plate in Flutter, Mode (1,1).

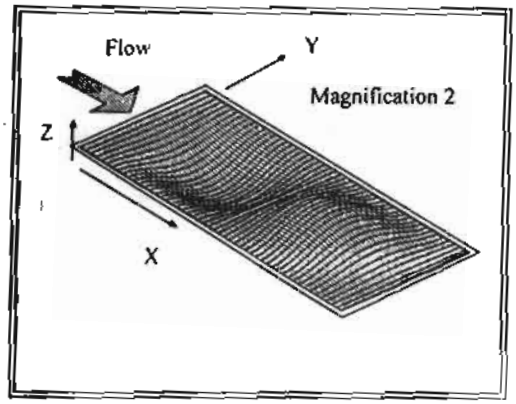

Fig. 10, Deflection of the Plate in Flutter, Mode (2, 1).

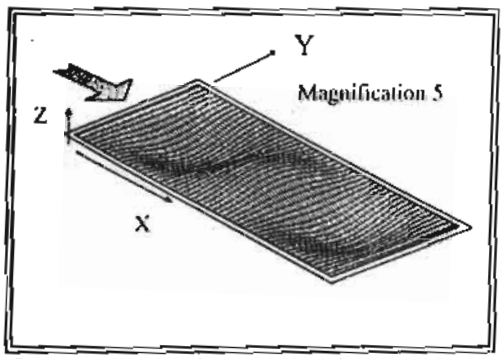

Fig. 11, Deflection of the Plate in Flutter, Mode (3, 1).

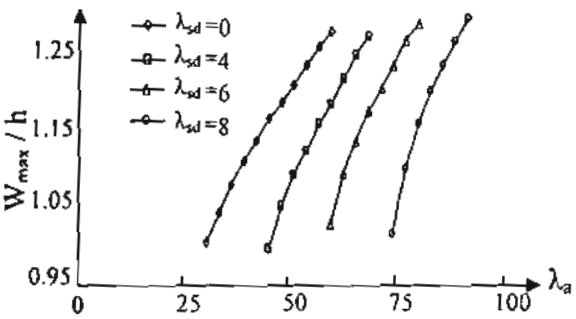

Fig. 12, Limit Cycle Amplitude vs. Dynamic Pressure for Different Values

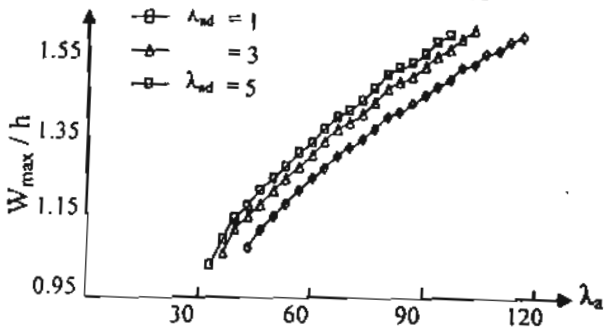

Fig. 13, Limit Cycle Amplitude vs. Dynamic Pressure for Different Values of the Nondimensional Aerodynamic Damping

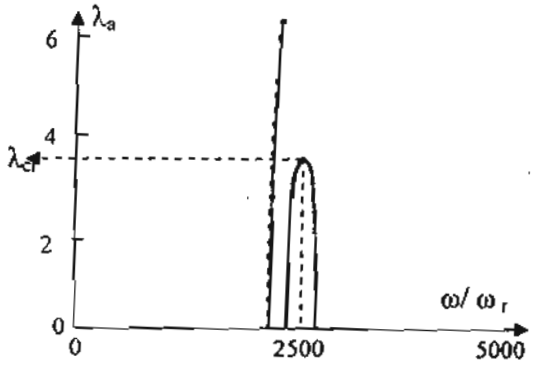

Fig. 14, Coaleascence of the Natural Frequencies at the Critical Aerodynamic

Fig. 15, Plate Supported from Rigid Base by Elastic Supports

Table 1, Values of α_m and γ_m in the Beam Eigen function or a Clamped Plate.

M	α_m	γ_m
1	4.730040744862704030	0.98250221457623807
2	7.853204624095837557	1.00077731190726905
3	10.99560783800167100	0.99996645012540900
4	14.13716549125746410	1.00000144989765650
5	17.27875965739948100	0.99999993734438300
6	20.42035224562061000	1.00000000270759500
m > 6	(2m+1) π/2	1.0

Table 2, Dimensions and Properties of the Plate

Length (m)	0.7620
Width (m)	0.1778
Thickness (x 10^{-3} m)	0.8128
Young's Modulus (x 10^{9} N/m^2)	72.398
Shear Modulus (x 10^{9} N/m^2)	27x10^{3}
Poisson's Ratio	0.3300
Density (x 10^{3} kg/m^3)	1.6189
Coefficient of Thermal Conductivity (μm/m.k)	11.700
Loss Factor	0.0050

Table 3, Experimental & Calculated Plate Frequencies for Different Boundary Conditions

Clamped	Simply Supported	Elastically Supported	Experimental Result
158	72	130.9	128
165	82	138.5	136-142
178	99	160.2	154-161
198	123	181.9	173-180
225	154	200.6	198-206
260	192	216.9	216-228
302	236	261.5	262-275
352	288	308.0	310-324